Theoretical and Applied Mechanics

25th AIMETA conference hosted by the Italian Association of Theoretical and Applied Mechanics in Palermo, Italy, September 4th - 8th, 2022

Edited by
Mario Di Paola
Livan Fratini
Fabrizio Micari
Antonina Pirrotta

MRF

Theoretical and Applied Mechanics
AIMETA 2022

Proceedings of the 25th AIMETA conference hosted by the Italian Association of Theoretical and Applied Mechanics in Palermo, Italy, September 4th - 8th, 2022.

https://pa22.aimeta.it/

Editors
Mario Di Paola, Livan Fratini, Fabrizio Micari, Antonina Pirrotta

Peer review statement

All papers published in this volume of "Materials Research Proceedings" have been peer reviewed. The process of peer review was initiated and overseen by the above proceedings editors. All reviews were conducted by expert referees in accordance with Materials Research Forum LLC high standards.

Copyright © 2023 by authors

Content from this work may be used under the terms of the Creative Commons Attribution 3.0 license. Any further distribution of this work must maintain attribution to the author(s) and the title of the work, journal citation and DOI.

Published under License by **Materials Research Forum LLC**
Millersville, PA 17551, USA

Published as part of the proceedings series
Materials Research Proceedings
Volume 26 (2023)

ISSN 2474-3941 (Print)
ISSN 2474-395X (Online)

ISBN 978-1-64490-242-4 (Print)
ISBN 978-1-64490-243-1 (eBook)

This book contains information obtained from authentic and highly regarded sources. Reasonable efforts have been made to publish reliable data and information, but the author and publisher cannot assume responsibility for the validity of all materials or the consequences of their use. The authors and publishers have attempted to trace the copyright holders of all material reproduced in this publication and apologize to copyright holders if permission to publish in this form has not been obtained. If any copyright material has not been acknowledged please write and let us know so we may rectify in any future reprint.

Distributed worldwide by

Materials Research Forum LLC
105 Springdale Lane
Millersville, PA 17551
USA
https://www.mrforum.com

Manufactured in the United State of America
10 9 8 7 6 5 4 3 2 1

Table of Contents

Preface
Committees

Fluid Mechanics

A novel one domain approach for free fluid-porous medium transport simulation - preliminary results
Costanza Aricò, Martin Schneider, Tullio Tucciarelli, Rainer Helmig 3

Solid Mechanics

Mechanical properties of cables made with helically wound carbon-nanotube fibers for advanced structural applications
Giovanni Migliaccio, Reginald DesRoches, Gianni Royer-Carfagni 11

A variational model for plastic reorientation in fibrous material: numerical experiments on phase segregation
Andrea Rodella, Antonino Favata, Stefano Vidoli 17

A coupled thermo-mechanical and neutron diffusion numerical model for irradiated concrete
Finite Element Method, Neutron Diffusion, Irradiated Concrete, Coupled Problem 23

Fracturing process in an anisotropic layered geomaterial: theoretical and computational predictions
Martina Rinaldi, Marco Trullo, Francesco Tornabene, Rossana Dimitri 29

A 3D visco-elasto-plasto damage constitutive model of concrete under long-term effects
Beaudin Freinrich Dongmo, Gianluca Mazzucco, Beatrice Pomaro, Jiangkun Zhang, Carmelo Majorana, Valentina Salomoni 34

A multiscale model for anisotropic damage and hysteresis in biodegradable polymers
Vitucci Gennaro, De Tommasi Domenico, Di Stefano Salvatore, Puglisi Giuseppe, Trentadue Francesco 41

Multiscale approach to decohesion in cell-matrix systems
Salvatore Di Stefano, Ariel Ramirez-Torres, Luca Bellino, Vincenzo Fazio, Gennaro Vitucci, Giuseppe Florio 47

One century of theoretical and applied mechanics of concrete and stone materials permeability. What have we learned?
Michela Monaco, Roberto Serpieri 53

Supercontraction of spider silks as a humidity-driven phase transition
Vincenzo FAZIO, Giuseppe FLORIO, Nicola Maria PUGNO, Giuseppe PUGLISI 59

Rate-dependent response of axonal microtubules and tau proteins under shear forces
Luca Bellino, Giuseppe Florio, Alain Goriely, Giuseppe Puglisi 65

A moving cohesive interface model for brittle fracture propagation
Umberto De Maio, Fabrizio Greco, Paolo Lonetti, Paolo Nevone Blasi, Andrea Pranno 71

A fractional-order theory of phase transformation in presence of anomalous heat transfer
Gianmarco Nuzzo, Fabiana Amiri, Salvatore Russotto, Emanuela Bologna, Massimiliano Zingales 77

Structural Mechanics

An accurate and refined nonlinear beam model accounting for the Poisson effect
E. Ruocco, J.N. Reddy 85

The extended membrane analogy for an engineered evaluation of the torsional properties of multi-material beams
Laura GALUPPI, Gianni ROYER CARFAGNI 91

Flexural tensegrity: Field applications
Claudio Boni , Gianni Royer-Carfagni 97

Structural designs that required thinking
Federico Bosetti, Massimo Maffeis, Gianni Royer-Carfagni 103

Fractional viscoelastic characterization of laminated glass
Luca Viviani, Mario Di Paola, Gianni Royer-Carfagni 109

A phase-field model for fracture in beams from asymptotic results in 2D elasticity
Giovanni Corsi, Antonino Favata, Stefano Vidoli 115

Static and free vibration analysis of anisotropic doubly-curved shells with general boundary conditions
Francesco TORNABENE, Matteo VISCOTI, Rossana DIMITRI 121

R-Funicularity of shells and effective eccentricity: Influence of tensile strength
Gloria Rita Argento, Stefano Gabriele, Valerio Varano 127

Tensile behaviour of rayon cords in different conditions
Lucas Pires da Costa, Giorgio Novati, Paola Caracino, Claudia Comi, Simone Agresti 133

Lower bound limit analysis through discontinuous finite elements and semi-analytical procedures
Zona Renato, Esposito Luca, Ferla Paolo, Palladino Simone, Totaro Elena, Vincenzo Minutolo 139

Finding damage in truss structures exploiting modal strains
Martina MODESTI, Antonio PALERMO, Cristina GENTILINI 145

Experimental analysis of new moment resisting steel connections
Salvatore Benfratello, Luigi Palizzolo, Santo Vazzano 151

Innovative devices for the protection of welded sections in steel structures
Salvatore Benfratello, Luigi Palizzolo and Santo Vazzano 157

Stress and strain fields in non-prismatic inhomogeneous beams
Giovanni Migliaccio 163

A simple procedure for the non-linear optimization of cable tension for suspended bridges
Ida MASCOLO, Mariano MODANO, Federico GUARRACINO 169

Mechanics of Machine

Experimental identification of a pneumatic valve-cylinder system for attitude control
Michele Gabrio ANTONELLI, Jacopo BRUNETTI, Walter D'AMBROGIO, Annalisa FREGOLENT, Francesco LATINI2 177

Performance evaluation of a Ball Screw mechanism through a multibody dynamic model
Antonio Carlo BERTOLINO, Andrea DE MARTIN, Massimo SORLI 183

Dynamic performance of an aerostatic pad with internal pressure control
Federico Colombo, Luigi Lentini, Terenziano Raparelli, Andrea Trivella 189

A novel prototype of diaphragm valve for passively compensated aerostatic pads
Federico Colombo, Luigi Lentini, Terenziano Raparelli, Andrea Trivella 195

Characterization of finger joints with underactuated modular structure
Gabriele Maria Achilli, Silvia Logozzo, Monica Malvezzi, Domenico Prattichizzo, Gionata Salvietti, Maria Cristina Valigi 201

On the effects of strain wave gear kinematic errors on the behaviour of an electro-mechanical flight control actuator for eVTOL aircrafts
Roberto Guida, Antonio C. Bertolino, Andrea De Martin, Andrea Raviola, Giovanni Jacazio, Massimo Sorli 207

Braking torque estimation through machine learning algorithms
Federico BONINI, Alessandro RIVOLA, Alberto MARTINI 213

Sizing and control system definition of an intelligent facility for qualification tests and prognostic research activities for electrical landing gear systems
Antonio Carlo Bertolino, Andrea De Martin, Giovanni Jacazio, Massimo Sorli 219

Novel approaches in computational mechanics

A mixed finite-element formulation for the elasto-plastic analysis of shell structures
Francesco S. LIGUORI, Antonio MADEO, Giovanni GARCEA 227

Geometrically nonlinear thermoelastic analysis of shells: modelling, incremental-iterative solution and reduction technique
F. LIGUORI, D. MAGISANO, L. LEONETTI,A. MADEO G. GARCEA 233

Extended virtual element method for elliptic problems with singularities and discontinuities in mechanics
Andrea CHIOZZI, Elena BENVENUTI, Gianmarco MANZINI N. SUKUMAR 239

An efficient plasticity-based model for reinforced concrete flat shells by a 4-nodes mixed finite element
Francesco S. LIGUORI, Antonella CORRADO, Antonio BILOTTA, Antonio MADEO 245

Automatic construction of structural meshes from photographic and laser surveys
Ivan PADUANO, Andrea MILETO, Egidio LOFRANO 251

An unconditionally stable time integration for the dynamics of elastic beams and shells in finite motions
Domenico MAGISANO, Leonardo LEONETTI,Giovanni GARCEA 257

Development of a multi-field computational tool for high-fidelity static aeroelastic simulations
Marco Grifò, Andrea Da Ronch, Alberto Milazzo, Ivano Benedetti 263

Numerical modeling of dynamic crack propagation mechanisms using a moving mesh technique based on the ALE formulation
Arturo Pascuzzo, Fabrizio Greco, Paolo Lonetti, Domenico Ammendolea, Giulia Sansone 267

Theoretical and applied biomechanics

A 3-year follow-up study on bone structure elastic quality
Francesca Cosmi, Simona Gentile, Sergio Carrato 275

Numerical simulation of coronary arteries blood flow: effects of the aortic valve and boundary conditions
Seyyed Mahmoud Mousavi, Gianluca Zitti, Marco Pozzi, Maurizio Brocchini 281

A limit analysis approach for the prediction of the human proximal femur ultimate load
Aurora Angela Pisano, Paolo Fuschi 287

The role of the interstitial fluid content in bone remodeling
Esposito Luca, Zona Renato, Palladino Simone, Minutolo Vincenzo, Fraldi Massimiliano 293

Fluid-structure interaction (FSI) analysis of 3D printing personalized stent-graft for aortic endovascular aneurysm repair (EVAR)
Sara Ragusa, Katia Siciliano, Francesco P. Di Simone, Salvatore Russotto, Emanuela Bologna, Massimiliano Zingales 299

Fractional diffusion of membrane receptors in endocytosis pathway
Gianmarco Nuzzo, Emanuela Bologna, Kaushik Dayal, Massimiliano Zingales 305

Masonry modelling and analysis: from material to structures

Some recent advances and applications in Distinct Element modelling of masonry structures
Mattia Schiavoni, Ersilia Giordano, Francesco Clementi 313

Sequential linear analysis of no-tension masonry structures
Grigor Angjeliu, Matteo Bruggi, Alberto Taliercio 319

Gaussian process emulation for rapid in-plane mechanical homogenization of periodic masonry
Luis C.M. da Silva, André Jesus, Gabriele Milani 325

Impacts analysis in the rocking of masonry circular arches
Paolo Bisegna, Simona Coccia, Mario Como, Nicola Nodargi 331

Numerical strategies for modelling masonry arch bridges strengthened with PBO-FRCM composites
Enrico Compagnone, Salvatore Gazzo, Leopoldo Greco, Massimo Cuomo, Loredana Contrafatto 337

Numerical procedure for detecting the optimal stress state within the profile of a cracked arch
Stefano Galassi, Giacomo Tempesta 343

Multiscale analysis of masonry vaults coupling shell elements to 3D-Cauchy continuum
Daniela Addessi, Paolo Di Re, Cristina Gatta, Elio Sacco 349

Vulnerability assessment of historical masonry buildings to excavation-induced settlements: palazzo assicurazioni generali
Daniela ADDESSI, Paolo DI RE, Achille PAOLONE 355

Pure compressive solutions for masonry domes under gravity loads
Arsenio Cutolo, Enrico Babilio, Ida Mascolo,, Elio Sacco 361

Dynamical systems and applications in civil and mechanical structures

Some remarks on the evaluation of work and dissipated energy associated with rate-independent hysteretic forces
Raffaele Capuano, Nicolò Vaiana, Luciano Rosati 369

Classification and modeling of uniaxial rate-independent hysteresis phenomena: some preliminary results
Nicolò Vaiana, Luciano Rosati 375

Materials with memory: some new results in viscoelastic models
Sandra CARILLO 381

Direct dynamics of 2D cable-driven parallel robots including cables mass effect and its influence in the control performance
Guillermo Rubio Gómez, Andrea Arena, Erika Ottaviano, Vincenzo Gattulli 387

On the dynamic stability of elastic structures subjected to follower forces
Francesca Levi, Angelo Carini 393

An inhomogeneous inelastic beam-like model for dynamic analyses of multistorey buildings
Ilaria FIORE, Annalisa GRECO, Salvatore CADDEMI Ivo CALIO' 399

Using multiple singular values in topology optimization of dynamic systems
Paolo Venini 405

The dynamics of circular arches with multiple damage
Francesco CANNIZZARO, Ilaria FIORE, Annalisa GRECO, Salvatore CADDEMI, Ivo CALIO' 411

A reduced hysteretic model of stockbridge dampers
Francesco Bogani, Alex Sosio, Francesco Foti, Luca Martinelli 417

Explicit expressions of the eigenfrequencies of damaged frames
Francesco CANNIZZARO, Salvatore CADDEMI, Ivo CALIO', Nicola IMPOLLONIA 423

Optimal design of single-degree-of-freedom vibro-impact system under harmonic base excitation
Giuseppe Perna, Maurizio De Angelis, Ugo Andreaus 429

Control and experimental dynamics

Friction-induced parametric oscillations in automotive drivelines: experimental analysis and modelling
Manuel Tentarelli, Stefano Cantelli, Silvio Sorrentino, Alessandro De Felice 437

Identification of normal modes of a set of strongly nonlinear springs
Francesco Latini, Jacopo Brunetti, Walter D'Ambrogio, Annalisa Fregolent 443

Complex dynamics in non-Newtonian fluid-structure interaction
F. Pellicano, A. Zippo, G. Iarriccio 449

The minimum variance distortionless response beamformer for damage identification using modal curvatures
Annamaria Pau, Ugurcan Eroglu 455

Experimental characterisation and numerical modelling of axially loaded wire rope isolators
Davide Pellecchia, Nicolò Vaiana, Salvatore Sessa, Francesco Marmo, Luciano Rosati 461

Continuous particle swarm optimization for model updating of structures from experimental modal analysis
Francesco LO IACONO, Giacomo NAVARRA, Calogero ORLANDO, Angela RICCIARDELLO 467

Shake-table test assessment of a base-isolation device for the seismic protection of the Goddess of Morgantina statue
Elena ALBERTI, Francesco LO IACONO, Giacomo NAVARRA 473

Microcontroller design for active vibration control
Antonio Zippo, Francesco Pellicano, Giovanni Iarriccio 479

Static and dynamic response analysis of stay cables using terrestrial laser scanning and vibration measurements
Cecilia Rinaldi, Marco Lepidi, Vincenzo Gattulli 485

Mechanical modelling of metamaterials and periodic structures

Stability domain and optimal design of a metamaterial made-up of a beam lattice with diagonal cables
Francesco Trentadue, Domenico De Tommasi, Gianluca Caramia, Nicola Marasciuolo 493

Two-scale asymptotic homogenization of hierarchical locally resonant metamaterials in anti-plane shear conditions
David Faraci, Claudia Comi, Jean-Jacques Marigo 499

A single-variable approach for layered beams with imperfect interfaces
Ilaria Monetto, Roberta Massabò 505

Microgeometrical design of lightweight bioinspired nacre-like composite materials for wave attenuation tuning
Andrea PRANNO, Fabrizio GRECO, Raimondo LUCIANO, Umberto DE MAIO 511

Anisotropic behaviours and strain concentration in lattice material evaluated by means of discrete homogenization
Salvatore Gazzo, Loredana Contrafatto, Leopoldo Greco, Massimo Cuomo 517

One-dimensional metastructures composed of cables with scatter masses: waves, vibrations and band gaps
Marco Moscatelli, Claudia Comi, Jean-Jacques Marigo 523

Graded meta-waveguides for elastic energy splitting
Luca Iorio, Jacopo M. De Ponti, Raffaele Ardito, Alberto Corigliano 529

Design of architected materials composed by periodic surfaces
Massimo Cuomo, Golshan Farzi, Roberto Ruggeri, Leopoldo Greco 535

Novel stochastic dynamics methodologies & signal processing techniques for civil engineering applications

A distributed analysis of vibration signals for leakage detection in Water Distribution Networks
Gabriele Restuccia, Ilenia Tinnirello, Fulvio Lo Valvo, Giacomo Baiamonte, Domenico Garlisi, Costantino Giaconia 543

Fractional differential equations under stochastic input processes handled by the improved pseudo-force approach
Alba Sofi, Giuseppe Muscolino, Mario Di Paola 549

Stochastic analysis of double-skin façades subjected to imprecise seismic excitation
Federica Genovese, Alba Sofi 555

Digital simulation of multi-variate stochastic processes
Salvatore Russotto, Mario Di Paola, Antonina Pirrotta 561

Identification of tie-rod properties in monumental buildings under uncertainty
Chiara Pepi, Mircea D. Grigoriu, Massimiliano Gioffrè 567

Open issues on procedures and methodologies for the vibration-based monitoring and dynamic identification of historic constructions

Post-earthquake continuous dynamic monitoring of the twin belfries of the Cathedral of Santa Maria Annunziata of Camerino, Italy
Gianluca Standoli, Francesco Clementi, Carmelo Gentile, Stefano Lenci 575

Deep learning for structural health monitoring: An application to heritage structures
Fabio Carrara, Fabrizio Falchi, Maria Girardi, Nicola Messina, Cristina Padovani, Daniele Pellegrini 581

Application of OMA technique to masonry slender towers: FEM updating and sensitivity analysis
Davide Li Rosi, Loredana Contrafatto, Salvatore Gazzo, Leopoldo Greco, Massimo Cuomo 587

A proposal of classification for machine-learning vibration-based damage identification methods
Francesca Marafini, Michele Betti, Gianni Bartoli, Giacomo Zini, Alberto Barontini, Nuno Mendes 593

Influence of a hemp biocomposite reinforcement on masonry vaults dynamic response
Massimiliano Gioffrè, Giacomo Navarra, Nicola Cavalagli, Francesco Lo Iacono, Roberta Scungio, Vittorio Gusella, Chiara Pepi 599

Modeling and analysis of nanocomposites and small-scale structures

Multiscale failure analysis of fiber-reinforced composite structures via a hybrid cohesive/volumetric nonlinear homogenization strategy
Daniele Gaetano, Fabrizio Greco, Lorenzo Leonetti, Paolo Nevone Blasi, Arturo Pascuzzo 607

Line element-less method (LEM) for arbitrarily shaped nonlocal nanoplates: exact and approximate analytical solutions
Alberto DI MATTEO, Antonina PIRROTTA 613

Perturbations for vibration of nano-beams of local/nonlocal mixture
Ugurcan Eroglu, Giuseppe Ruta 619

Reaction-diffusion-drift equations and gradient flows in mechanics and continuum physics

An effective strategy to transform second-gradient equilibrium equations from the Eulerian to the Lagrangian configuration
Roberto Fedele, Francesco dell'Isola, Pierre Seppecher, Simon R. Eugster 627

New frontiers in multibody systems vibration analysis

A simple tool to forecast the natural frequencies of thin-walled cylinders
Marco Cammalleri, Antonella Castellano, Marco Abella 635

Multibody dynamics modeling of drivetrain components: On the caged-roller dynamics of centrifugal pendulum vibration absorbers
Mattia Cera, Marco Cirelli, Luca D'Angelo, Ettore Pennestrì, Pier Paolo Valentini 641

Modal analysis of a four-bar linkage MEMS microgripper with co-operative electrostatic actuation
Andrea Rossi, Nicola Pio Belfiore 647

Interface reduction in flexible multibody systems
Alessandro CAMMARATA, Pietro Davide MADDÌO, Rosario SINATRA 653

Dynamic analysis of lightweight gears through multibody models with movable teeth
Marco Cirelli, Alessio Cellupica, Mattia Cera, Oliviero Giannini, Pier Paolo Valentini, Ettore Pennestrì 659

Surface error correction of a mesh deployable reflector
Pietro Davide MADDIO, Pietro SALVINI, Rosario SINATRA, Alessandro CAMMARATA 665

Multibody simulations of a distributed-compliance helical transmission joint for largely misaligned shafts
Sorgonà Orazio, Giannini Oliviero, Cirelli Marco, Pier Paolo Valentini 671

Mechanics of renewable energy systems

Combining pendulum and gyroscopic effects to step-up wave energy extraction in all degrees of freedom
Giuseppe Giorgi, Fabio Carapellese, Mauro Bonfanti, Sergej Antonello Sirigu 679

On the manipulation of the magnetic forces for improving the contactless plucking in piezoelectric vibration energy harvesters
Michele Rosso, Filippo Pietro Perli, Alberto Corigliano, Raffaele Ardito 685

First offshore windfarm in the Mediterranean Sea - Italy
Luigi Severini, Alessandro Severini, Sara Bray, Simona Capozza 691

Advances in mathematical modeling and experimental techniques for quantification and prediction of fluid dynamic noise

Multi-modal noise generation in low Mach number orifice plates: an experimental investigation
Luca Nicola QUARONI, Islam RAMADAN, Simon RAMPNOUX, Stefano MALAVASI, Emmanuel PERREY-DEBAIN 699

Advanced process mechanics

Milling of alumina-based ceramic foams: tool material effects
Giovanna Rotella, Maria Rosaria Saffioti, Michela Sanguedolce, Flaviano Testa, Luigino Filice, Fabrizio Micari 707

Progresses in multi-materials billet manufacturing out of metal scraps through friction stir consolidation
Abdul Latif, Giuseppe Ingarao, Livan Fratini, Fabrizio Micari 713

Process mechanics in continuous friction stir extrusion process of aluminum alloy
Gianluca Buffa, Davide Campanella, Livan Fratini, Adnan Muhuammed, Fabrizio Micari 719

Keyword index

Materials Research Proceedings **26** (2023) 429-434 https://doi.org/10.21741/9781644902431-70

Optimal design of single-degree-of-freedom vibro-impact system under harmonic base excitation

Giuseppe Perna[1,a*], Maurizio De Angelis[1,b] and Ugo Andreaus[1,c]

[1] Department of Structural and Geotechnical Engineering, Sapienza University of Rome, Via Eudossiana 18, Rome, 00148, Italy

[a]giuseppe.perna@uniroma1.it, [b]maurizio.deangelis@uniroma1.it, [c]ugo.andreaus@uniroma1.it

Keywords: Vibro-Impact Systems, Dynamic Response Control, Bumper, Gap, Numerical Modeling, Harmonic Base Excitation

Abstract. Strong seismic excitations can induce considerable displacements in base-isolated structures. These may in turn cause damage to the isolation system or impacts against adjacent structures in the event of an insufficient seismic gap. A strategy of reducing displacements can be achieved through the interposition, between the isolated structure and adjacent structures, of deformable and dissipative devices, called bumpers. In this paper, the response of single-degree-of-freedom (SDOF) base-isolated systems subjected to sine excitations and whose displacements are limited by optimally designed bumpers are analyzed, the bumpers being designed according to an optimal design criterion.

Introduction

One of the most widely used strategies for passive control of the dynamic response of sensitive structures and equipment is base isolation. This strategy consists of interposing a highly horizontally deformable element between the base floor and the structure (or equipment), so that the period of the system is increased significantly resulting in a reduction of the transmitted acceleration. However, strong earthquakes can cause large displacements at the isolated floor level, exceeding its limit deformation, or induce impacts with adjacent elements. Rigid impact causes significant increases in acceleration and floor drifts that can cause serious damage to both structural and nonstructural elements [1].

An effective strategy to reduce and control the adverse effects due to large isolation floor displacements is the interposition of deformable and dissipative devices, called bumpers. Various experimental investigations have been conducted by the authors on the influence of bumpers on the dynamic response of single-degree-of-freedom (SDOF) systems subjected to sine base excitation [2-4]. From these studies, it was observed that the parameters governing the impact between system and bumper can be identified by three elements: gap (distance between mass and bumper), stiffness and damping of the bumper. The authors, moreover, based on the experimental investigations defined a numerical model that allowed the identification of optimality relations between bumper stiffness, bumper damping coefficient and gap, reducing the design of such a control strategy to a single parameter [3-7].

This paper analyzes the response obtained from a numerical model of SDOF system constrained by two bumpers, arranged symmetrically on both sides of the mass of the system with an initial gap, subjected to sine excitation. The design of bumpers is done in accordance with the optimality relationship [6] and the optimal design curve [7]. The absolute maximum values of the response in absolute mass acceleration and relative mass displacement are represented as a function of frequency ratio and for six initial gaps. All results shown are represented in dimensionless terms so that they can be generalized.

The text is organized as follows: the first paragraph introduces the model and its equations of motion; the second paragraph explains the optimal design criterion that is used to identify the

Content from this work may be used under the terms of the Creative Commons Attribution 3.0 license. Any further distribution of this work must maintain attribution to the author(s) and the title of the work, journal citation and DOI. Published under license by Materials Research Forum LLC.

Materials Research Proceedings **26** (2023) 429-434 https://doi.org/10.21741/9781644902431-70

parameters governing the impact; the third paragraph reports the results of the numerical analysis; and finally, the fourth paragraph reports the conclusions and possible future developments of the work.

Model and equations of motion

The model adopted in the numerical analyses is shown in Fig. 1. The figure represents a vibro-impact single-degree-of-freedom (SDOF) system that consists of a mass M, a damper D and two deformable and dissipative obstacles, arranged symmetrically on both sides of the mass with an initial gap G_{0j} (j=R right side, j=L left side) and denoted as right bumper B_R and left bumper B_L, respectively. The damper and the bumpers are modeled by a linear elastic element, with stiffness K and K_j *(j=R,L)*, respectively, and a linear viscous dashpot, with damping coefficient C and C_j *(j=R,L)*, respectively, arranged in parallel. The system is subjected by a sine base acceleration $A_t(t) = A_G sin(\Omega t)$, where A_G is the amplitude and Ω in the circular frequency of this excitation. Finally, in figure 1 $u(t)$ refers to the relative displacement of the mass with respect to the ground, and $u_j(t)$ *(j=R,L)* refers to the deformation of the bumper.

The equations of motion were written in dimensionless form to make them as general as possible. The components of the equation were normalized with respect to $F^* = M\omega^2 u^*$, which represents the maximum force in the SDOF system in free flight (without obstacles, FF): the quantity $u^* = u_{st} R_{d,max}$ represents the maximum relative displacement in FF, where $u_{st} = A_G/\omega^2$ is the static displacement and $R_{d,max} = 1/(2\xi\sqrt{1-\xi^2})$ is the maximum value of the dynamic amplification factor $R_d(\xi, \beta)$; while $\omega = \sqrt{K/M}$ denotes the frequency of the system. The frequency ratio $\beta = \Omega/\omega$ and the damping ratio $\xi = C/(2M\omega)$, are introduced and the dimensionless time $\tau = \omega t$ is defined. In the dimensionless equations, the quantities $q = u/u^*$ and $q_j = u_j/u^*$ *(j=R,L)* are the dimensionless displacement of the mass and dimensionless deformation of the bumper, respectively. Similarly, the dimensionless gap is $\delta_{0j} = G_{0j}/u^*$ *(j=R,L)* and can take values comprised within the range $0 \le \delta_{0j} \le 1$. Finally, $f(\tau) = 2\xi q'(\tau) + q(\tau)$ is the damper dimensionless force, $f_j(\tau) = 2\xi\gamma_j q'_j(\tau) + \lambda_j q_j(\tau)$ with (j=R,L) –where $\gamma_j = C_j/C$ and $\lambda_j = K_j/K$– as the dimensionless contact forces, and $a_G = 2\xi\sqrt{1-\xi^2}$ as the dimensionless amplification of the dimensionless sine excitation $a_t(\tau)$.

Thus, the motion equations of the model can be written in the following dimensionless form:

$$\begin{cases} q''(\tau) + f(\tau) + f_j(\tau) \cdot \psi_1[\delta_j(\tau)] \cdot \psi_2[f_j(\tau)] = -a_G sin\beta\tau \\ f_i(\tau) = 0 \end{cases}; \quad (1)$$

where it is assumed that if the mass is in contact with the left bumper, then j=L and i=R, or if the mass is in contact with the right bumper, then j=R and i=L. In the equations the Heaviside functions ψ_1 and ψ_2 are defined as follows:

$$\text{contact} \quad \psi_1[\delta_j(\tau)] = \begin{cases} 0, & \delta_j(\tau) > 0 \\ 1, & \delta_j(\tau) = 0 \end{cases} \quad (j = R, L); \quad (2)$$

$$\text{separation} \quad \psi_2[f_j(\tau)] = \begin{cases} 0, & f_R(\tau) \le 0 \quad or \quad f_L(\tau) \ge 0 \\ 1, & f_R(\tau) > 0 \quad or \quad f_L(\tau) < 0 \end{cases}; \quad (3)$$

where $\delta_j(\tau)$ *(j=R,L)* represents the gap function in terms of the dimensionless time τ and, if j=R, is equal to $\delta_R(\tau) = \delta_{0R} + q_R(\tau) - q(\tau)$, and, if j=L, is equal to $\delta_L(\tau) = \delta_{0L} - q_L(\tau) + q(\tau)$. In all the equations introduced the apex (′) denotes differentiation with respect to the dimensionless time τ.

Because the bumpers are equal and arranged symmetrically on both sides of the mass $\gamma_R = \gamma_L = \gamma$, $\lambda_R = \lambda_L = \lambda$ and $\delta_{0R} = \delta_{0L} = \delta_0$.

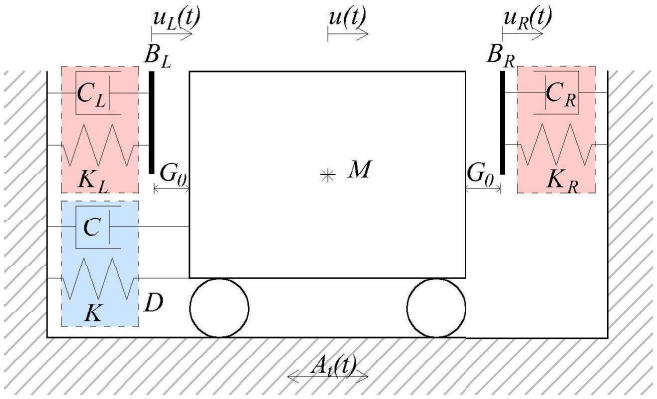

Fig. 1. ***Model of the vibro-impact system.***

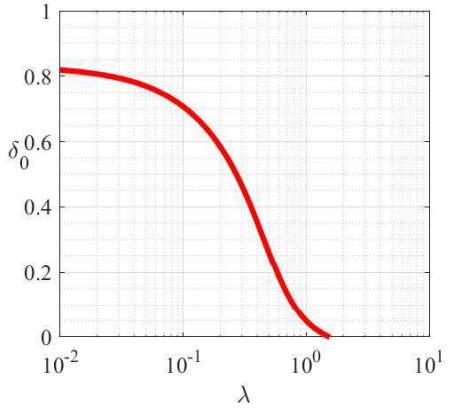

Fig. 2. ***Optimal design curve of the bumper.***

Optimal design of the bumpers

In order to optimize the control of the dynamic response of the system, the physical parameters governing the impact (gap δ_0, stiffness λ and damping γ of the bumper) to be adopted are obtained in relation to an optimal design criterion based on a relationship that links damping ratio ξ of the system with parameters λ and γ of the bumpers [6], and on a curve in which bumper stiffness λ is identified in relation to the gap δ_0 [7].

The optimality relationship is defined as follows:

$$\frac{\gamma}{\lambda} = \frac{1}{2\xi}. \tag{4}$$

This relationship was obtained by a parametric analysis in which, for each investigated δ_0, and for fixed values of ξ and of γ, the value of λ was searched such that the peak acceleration of the mass in the primary resonance is minimized. This is possible because the bumper is fully exploited: the bumper has sufficient time to recover its deformation before the next impact, dissipating all the deformation energy accumulated up to then, and it does not remain inactive because the next impact occurs practically immediately after recovery.

The optimality relationship (4) is independent of the gap and, through this relationship, it is possible to reduce the number of impact parameters from three, which in dimensionless terms can be identified as δ_0, λ and γ, to two, since by choosing λ we obtain the value of the corresponding γ.

With the introduction of the optimal curve an additional constraint is introduced, reducing the bumper design to one parameter, the dimensionless gap δ_0. The optimal design curve, shown in Fig. 2, associates to each δ_0 a pair of values λ and γ (Eq. 4), which minimizes the peak absolute acceleration of the mass in primary resonance and therefore the force acting on the mass.

Looking at the red curve in figure 2, it is clear how the control over the response of vibro-impact system with a dimensionless gap $\delta_0 > 0.82$, is ineffective. This is because, for these values of δ_0, the optimal stiffness ratio λ is so small that the presence of the bumpers is negligible.

Analysis of numerical response

In this paragraph, the numerical responses of the model characterized as follows are analyzed: the damping ratio of the damper is $\xi = 0.10$, the bumper parameters λ and γ are designed in accordance with the optimality relationship (4) and the optimal design curve (Fig.2). The represented response quantities are dimensionless excursion of the absolute acceleration and of the relative displacement, of the mass, both normalized with respect to two different factors:

$$\eta_{a1} = \frac{\Delta\alpha}{\Delta\alpha_0},\ \eta_{a2} = \frac{\Delta\alpha}{\Delta\alpha_t}, \eta_{d1} = \frac{\Delta q}{\Delta q_0},\ \eta_{d2} = \frac{\Delta q}{\Delta q_t}, \tag{5}$$

Materials Research Proceedings **26** (2023) 429-434 https://doi.org/10.21741/9781644902431-70

where $\alpha = a_t + q''$, the dimensionless quantities whit subscript ($_o$) are related to the case of free flight in resonance (FF) and the dimensionless quantities whit subscript ($_t$) are related to the ground. The excursion ($\Delta i, i = \alpha, q$) was calculated as the difference between the maximum and minimum values recorded at steady state of each sub-frequency range.

Figures 3 show the normalized quantities analyzed as a function of the frequency ratio β and in the terms of six dimensionless gaps $\delta_0 = 1, 0.5, 0.3, 0.2, 0.1, 0$, where $\delta_0 = 1$ represents the FF and $\delta_0 = 0$ the case of mass adjacent with bumper.

The curves in Fig. 3a-3b represent the Pseudo-Resonance Curves (PRCs) of the dimensionless absolute acceleration of the mass, normalized in (a) with respect to the FF, and in (b) with respect to the ground. The black curves reproduce dimensionless excursion of the absolute acceleration of the mass in FF, subjected to the dimensionless sine excitation a_t. The curve $\eta_{a1_{FF}}(\beta)$ starts from the value $\eta_{a1_{FF}}(0) \simeq 0.20$ and then attains a peak at resonance, for $\beta = \sqrt{1-2\xi^2} \simeq 0.99$, equal to 1. Once the peak has been passed, for increasing β the acceleration $\eta_{a1_{FF}}$ tends to 0. The curve $\eta_{a2_{FF}}(\beta)$ starts from value 1 ($\beta = 0$), reaches the resonance peak at $\beta = \sqrt{1-2\xi^2} = 5.12$, and, for increasing values of β, $\eta_{a2_{FF}}$ decreases tending to 0 for β tending to infinity. The red dashed curves represented the cases with impact (thinner dashes imply smaller values δ_0). The study of Fig. 3a-3b shows that the curves $\eta_{a1}(\beta)$ are scaled by TR_{max}, that is the maximum value of the resonance transmissibility, relative to curves $\eta_{a2}(\beta)$, so the comments will be unique for both two types of curves, with percentage changes. In Fig. 3a-3b, as δ_0 decreases, a reduction and a shift toward larger β of the acceleration peaks are observed. The lowest value of the peak occurs in the case $\delta_0 = 0$, where a 62% reduction of the maximum acceleration value is obtained with respect to FF. The other cases show a reduction of 48% for $\delta_0 = 0.1$, 30% for $\delta_0 = 0.2$, 22% for $\delta_0 = 0.3$ and 9% for $\delta_0 = 0.5$. The β of resonance increases from 0.99 in the FF to 1.02 for $\delta_0 = 0.5$, 1.09 for $\delta_0 = 0.3$, 1.15 for $\delta_0 = 0.2$, 1.24 for $\delta_0 = 0.1$ up to 1.66 for $\delta_0 = 0$. The dashed curves, for some values of β, overlap with the FF curve: this is because for those values of β and for the value of δ_0 relative to that dashed curve, impact does not occur. The only case in which impact always occurs is the case of mass adjacent to bumpers ($\delta_0 = 0$), which, for $\beta > 1.25$, reports larger accelerations than FF and, for $\beta > 1.52$, larger than the other cases. For the other δ_0 investigated, the acceleration turns out to be greater than FF in a small range of β, between 1.04 and 1.72.

Fig. 3c-3d shows the PRCs of the dimensionless relative displacement of the mass, normalized with respect to FF, in (c), and with respect to the ground, in (d). The black curves represent the dimensionless excursion of the relative displacement of the mass in FF, subjected to the dimensionless sine excitation a_t. The dimensionless displacement curve in FF $\eta_{d1_{FF}}(\beta)$, reports the maximum at $\beta = \sqrt{1-2\xi^2} \simeq 0.99$, in which it takes value 1. For β between 0, in which $\eta_{d1_{FF}}(0) \simeq 0.20$, and $\sqrt{1-2\xi^2}$, $\eta_{d1_{FF}}$ grows as β increases. Passing the peak value, for increasing β the displacement $\eta_{d1_{FF}}$ decreases, tending, in the limit, to the value 0. The dimensionless displacement in FF, $\eta_{d2_{FF}}(\beta)$, reports the maximum in $\beta = 1/\sqrt{1-2\xi^2} \simeq 1.01$ of intensity equal to 5.03. In the first range between 0 and β relative to the maximum, $\eta_{d2_{FF}}$ has an increasing monotonic trend, after which, as β increases, it decreases tending, for infinite β, to the value 1 (maximum ground displacement). In contrast to $\eta_{d1_{FF}}$, $\eta_{d2_{FF}}$ at $\beta = 0$ assuming zero value.

The red dashed curves show the displacement responses of the impacted cases (thinner dashes imply smaller values of δ_0). Referring to Fig. 3c, the peaks of displacements, as δ_0 decreases, move toward larger β and decrease. With respect to FF ($\delta_0 = 1$), η_{d1} decreases by 90% for $\delta_0 = 0$, by 69% for $\delta_0 = 0.1$, by 55% for $\delta_0 = 0.2$, by 42% for $\delta_0 = 0.3$, and by 22% for $\delta_0 = 0.5$, while the β relative to these maximum values turns out to be 1.59, 1.19, 1.13, 1.09, and 1.03,

Materials Research Proceedings **26** (2023) 429-434 https://doi.org/10.21741/9781644902431-70

respectively. Each curve related to $\delta_0 \geq 2\,\xi\sqrt{1-\xi^2}$ ($\simeq 0.2$) is initially coincident with the FF case, until η_{d1}, growing, reaches the value δ_0, causing the impact to occur because the displacement in FF is greater than the gap. Conversely, once the value of β has been exceeded beyond which $\eta_{d1_{FF}} \leq \delta_0$, the curve for that value of δ_0 turns out to coincide with the FF case. The only curve that shows a single point of coincidence with free flight is the one related to $\delta_0 = 0$, for $\beta = 1.75$; this curve also, for $\beta < 1.75$, shows smaller values than for FF, while for $\beta > 1.75$ larger values, with a maximum increase of 28% in displacement value in FF case. The PRCs for the other values of $\delta_0 > 0$ exhibit larger values than FF for $1.27 < \beta < 1.72$ with $\delta_0 = 0.1$, for $1.18 < \beta < 1.40$ with $\delta_0 = 0.2$, for $1.13 < \beta < 1.27$ with $\delta_0 = 0.3$, and for $1.07 < \beta < 1.15$ with $\delta_0 = 0.5$ with maximum increases of 33% (for $\beta = 1.5$), 24% (for $\beta = 1.3$), 18% (for $\beta = 1.2$), and 7% (for $\beta = 1.12$). In Fig. 3c, as δ_0 decreases, there is, as in Fig. 3d, a shift to the right and a reduction of peak displacement whit respect to FF, but at different dimensionless frequencies β and with different percentage reduction: for $\delta_0 = 0$ the peak is for $\beta = 2.04$ with 68% reduction, for $\delta_0 = 0.1$ the peak is for $\beta = 1.35$ with 50% reduction, for $\delta_0 = 0.2$ the peak is for $\beta = 1.22$ with 38% reduction, for $\delta_0 = 0.3$ the peak is for $\beta = 1.15$ with 28% reduction, and for $\delta_0 = 0.5$ the peak is for $\beta = 1.07$ with 13% reduction. As observed in Fig. 3c-3d, the response for $\delta_0 = 0$ never coincides with the FF curve except at $\beta = 1.75$.

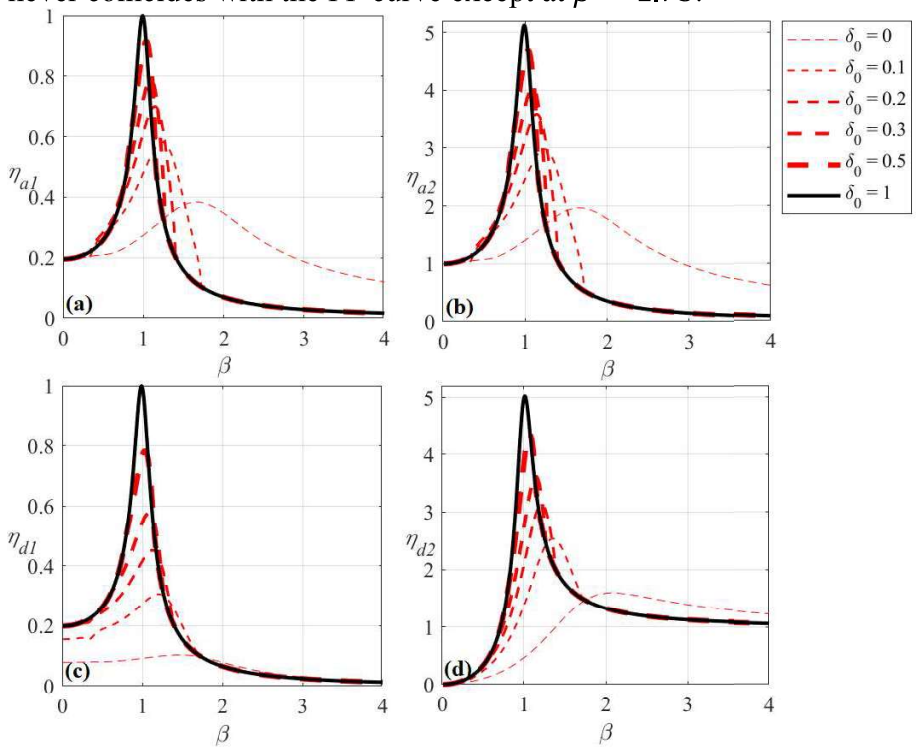

Fig. 3. PRCs of dimensionless acceleration: (a) PRC of $\eta_{a1}(\beta)$; (b) PRC of $\eta_{a2}(\beta)$; and PRCs of dimensionless displacement: (c) PRC of $\eta_{d1}(\beta)$; (d) PRC of $\eta_{d2}(\beta)$. The curves are related to different values of δ_0: in black δ_0=1 (FF), in dashed red δ_0=0.5, 0.3, 0.2, 0.1, 0 (lower thicknesses represent lower δ_0).

Conclusions and future developments

In this paper, the numerical dynamic response of the SDOF system, subjected to sine excitation, constrained by two symmetrically arranged deformable and dissipative bumpers designed with optimality relation (4) and optimal design curve (Fig. 2) is analyzed. Six different values of the design parameter δ_0 (dimensionless gap) are considered: two extreme cases, $\delta_0 = 1$, a touching condition between mass and bumpers representative of FF, and $\delta_0 = 0$, a condition with mass adjacent to the bumpers; and intermediate cases, $\delta_0 = 0.5$, $\delta_0 = 0.3$, $\delta_0 = 0.2$ and $\delta_0 = 0.1$.

The response quantities which have been analyzed are the absolute acceleration of the mass and the relative displacement of the mass with respect to the ground, normalized with respect to both (i) the peak values of acceleration and displacement in FF, and (ii) the peak values of base

acceleration and ground displacement. It was found that as δ_0 decreases, the maximum values of peak acceleration and displacement undergo greater reductions with respect to FF, reporting in the case $\delta_0 = 0$ the greatest reductions (peak of acceleration reduced by 62% for both $\eta_{a1}(\beta)$ and $\eta_{a2}(\beta)$, peak of displacement reduced by 90% for $\eta_{d1}(\beta)$, and by 68% for $\eta_{d2}(\beta)$). However, the case $\delta_0 = 0$ reports larger values of acceleration for $\beta > 1.52$, compared with the other cases examined. A phenomenon of increased displacement, due to the presence of bumper, was also observed for some β following the primary resonance in FF ($1.08 < \beta < 1.15$ for $\delta_0 = 0.5$, $1.13 < \beta < 1.27$ for $\delta_0 = 0.3$, $1.18 < \beta < 1.4$ for $\delta_0 = 0.2$, $1.27 < \beta < 1.71$ for $\delta_0 = 0.1$, $\beta > 1.72$ for $\delta_0 = 0$). This phenomenon is named bouncing-effect in the literature.

These results show that the adoption of this optimal design criterion and an appropriate choice of the gap parameter δ_0 allow beneficial effects in mitigating the dynamic response to be gained. Thus, the need emerges to extend this study to cases of real dynamic actions, such as earthquakes, and evaluate the effects of appropriately designed dissipative and deformable bumpers on systems subjected to different seismic excitations.

References

[1] P.C. Polycarpou, P. Komodromos, On poundings of a seismically isolated building with adjacent structures during strong earthquakes, Earthq. Eng. Struct. Dyn. 39 (2010). https://doi.org/10.1002/eqe.975

[2] U. Andreaus, M. De Angelis, Influence of the characteristics of isolation and mitigation devices on the response of single-degree-of-freedom vibro-impact systems with two-sided bumpers and gaps via shaking table test, Struct. Control Health Monit. 27(2020). https://doi.org/10.1002/stc.2517

[3] G. Stefani, M. De Angelis, U. Andreaus, Scenarios in the experimental response of a vibro impact single-degree-of freedom systems and numerical simulations, Nonlinear Dyn. 103 (2021). https://doi.org/10.1007/s11071-020-05791-4

[4] G. Stefani, M. De Angelis, U. Andreaus, Influence of the gap size on the response of a single-degree-of-freedom vibro-impact system with two-sided constraints: Experimental tests and numerical modeling, Int. J. Mech. Sci. 206 (2021). https://doi.org/10.1016/j.ijmecsci.2021.106617

[5] G. Stefani, M. De Angelis, U. Andreaus, Numerical study on the response scenarios in a vibro-impact single-degree-of-freedom oscillator with two unilateral dissipative and deformable constraints, Commun. Nonlinear Sci. Numer. Simul. 99 (2021). https://doi.org/10.1016/j.cnsns.2021.105818

[6] G. Stefani, M. De Angelis, U. Andreaus, The effect of the presence of obstacles on the dynamic response of single-degree-of-freedom systems: Study of the scenarios aimed at vibration control, J. Sound Vib. 531 (2022). https://doi.org/10.1016/j.jsv.2022.116949

[7] G. Stefani, M. De Angelis, U. Andreaus, Exploit the study of the scenarios for the control of the response of single-degree-of-freedom systems with bumpers, Submitted to Eng. Struct. (2022).